Magazine of Civil Engineering

ISSN 2712-8172

journal homepage: http://engstroy.spbstu.ru/

Research article

UDC 624

DOI: 10.34910/MCE.141.6

Properties of concrete incorporating treated prickly pear fibers

I. Tarkhani[1], ***Z. Kammoun***[2,3] ✉, ***A. Trabelsi***[1 2], ***H. Smaoui***[4]

[1] *LGC for National Engineering School of Tunis (ENIT), University of Tunis El Manar, Tunis, Tunisia*

[2] *Military Academy of Fondouk Jedid, Nabeul, Tunisia*

[3] *GESTE for National School of Engineers of Sfax, University of Sfax, Sfax, Tunisia*

[4] *Faculty of Engineering. King Abdulaziz University, Jeddah, Kingdom of Saudi Arabia*

✉ *kammounzied@yahoo.fr*

Keywords: concrete, prickly pear, fiber, treatment, long-term, strength, mechanical properties, thermal properties

Abstract. The integration of natural fibers into building materials is key to enhancing sustainability within the construction industry. However, vegetable fibers are known to undergo mechanical degradation over time when embedded in the alkaline environment of cementitious matrices. This study investigates the incorporation of prickly pear fibers into concrete, evaluating the efficacy of three surface treatments (epoxy, lime, and bitumen) over a curing period extending from 3 to 180 days. Results indicate that while untreated fibers reduce compressive strength, the applied treatments significantly mitigate this loss. Notably, epoxy-treated fiber concrete exhibited only an 11 % decrease in compressive strength at 28 days compared to ordinary concrete, eventually achieving a strength 53 % higher than that of untreated fiber concrete by 180 days. At the optimal dosage of 15 kg/m^3, epoxy treatment enhanced 28-day flexural strength by 333 %, while lime treatment yielded a 229 % increase. Furthermore, whereas untreated fibers exhibited mechanical degradation after 28 days, treated fibers demonstrated sustained strength gains up to 180 days. Additionally, a fiber dosage of 40 kg/m^3 substantially improved thermal performance, reducing conductivity by 40–45 % and increasing specific heat capacity by 22–24 %. These findings highlight the potential of treated prickly pear fibers as a viable, sustainable reinforcement for high-performance construction applications.

Citation: Tarkhani, I., Kammoun, Z., Trabelsi, A., Smaoui, H. Properties of Concrete Incorporating Treated Prickly Pear Fibers. Magazine of Civil Engineering. 2026. 19(1). DOI: 10.34910/MCE.141.6

1. Introduction

Plant fibers are increasingly incorporated into cementitious materials owing to their renewability, biodegradability, low embodied energy, and near carbon-neutral life cycle [1]. Beyond these environmental benefits, their low density and cost-competitiveness relative to synthetic fibers make them attractive for lightweight, sustainable construction [2, 3]. Numerous plant-based reinforcements – including straw, date palm, Stipa tenacissima (Alfa), bamboo, sisal, coconut shell, and Ampelodesmos mauritanicus (Diss) – have been evaluated in concrete and mortar composites [4–12]. A consistent finding across the literature is a reduction in composite density, primarily due to the lower intrinsic density of lignocellulosic materials compared to mineral aggregates. In parallel, several studies report enhanced thermophysical performance, specifically reductions in thermal conductivity, diffusivity, and effusivity, alongside increased specific heat capacity. These effects are attributed both to the low intrinsic thermal conductivity of plant fibers and the additional porosity introduced within the matrix [1].

Mechanical performance is highly dependent on fiber morphology, dosage, dispersion, and the quality of the fiber–matrix interface. Although compressive strength often declines with increasing fiber content – largely due to higher porosity and interfacial weaknesses – improvements in flexural strength, splitting tensile strength, and post-cracking toughness are frequently observed. Alfa fiber-reinforced concrete, for example, exhibited reduced compressive strength at high dosages, yet flexural and tensile strengths peaked at 15 kg/m^3, accompanied by improved ballistic resistance [13]. Similarly, incorporating 50 mm maguey fibers pretreated with calcium oxide (0.9 % by cement weight) increased compressive, flexural, and tensile strengths by 13.4, 17.4, and 1.5 %, respectively, while boosting the modulus of elasticity by 53.8 % [14]. In ultra-high-performance concrete, sisal fibers (6–18 mm, 1–3 % by volume) had negligible effects on compressive strength but successfully transitioned the failure mode from brittle to ductile; at a 2 % volume fraction, flexural strength and toughness increased by 16.7 and 540 %, respectively [15]. Comparable trends were observed with palm leaf sheath fibers, whereas banana fibers led to performance losses attributed to inadequate interfacial bonding [16].

Among various lignocellulosic reinforcements, prickly pear fibers exhibit significant structural and thermal potential. In lightweight concrete, their incorporation reduced density by approximately 25 % and thermal conductivity by 42 %, while increasing flexural strength by 170 %; compressive strength remained above 22 MPa, thereby meeting structural-grade requirements [17]. In high-strength concrete, density reductions of up to 30 % and thermal conductivity decreases of 50 % were reported, with compressive strengths ranging from 41 to 59 MPa and flexural strength gains reaching 35 % at 28 days [18]. Furthermore, improved impact resistance and toughness highlight their suitability for both conventional and high-performance systems.

Despite these advantages, long-term durability remains a critical challenge. Plant fibers consist primarily of cellulose, hemicellulose, and lignin, all of which are susceptible to degradation in the highly alkaline cementitious environment (pH > 12). Alkaline hydrolysis of hemicellulose and lignin, partial depolymerization of cellulose chains, and the diffusion of pore solution toward the fiber surface progressively weaken the lignocellulosic structure. Moreover, the precipitation of hydration products within the lumen and cell walls promotes stiffening and embrittlement, while cyclic swelling and shrinkage of the hydrophilic fibers under fluctuating moisture conditions induce interfacial microcracking [19, 20]. Collectively, these mechanisms compromise long-term strength and toughness.

To mitigate degradation and enhance fiber–matrix compatibility, several pretreatment strategies have been explored. Lime treatment of palm nut shells increased 28-day compressive strength by 10 %, whereas polyvinyl alcohol (PVA) primarily reduced water absorption without providing mechanical benefits [21]. Boiling and linseed oil coating of Diss fibers improved tensile behavior and delayed crack initiation [22]. A 60-minute $Ca(OH)_2$ treatment of date palm fibers enhanced flexural strength by removing inhibitory extractives and promoting interfacial bonding [23]. Mineral and organic coatings have also been investigated to control dimensional instability: oil impregnation reduced drying shrinkage in wood-based composites by 43.6 %, while lime coatings improved compatibility more effectively than cement [24]. Paraffin wax coatings acted as hydrophobic barriers to optimize moisture exchange, whereas prolonged pre-wetting (48 h) reduced performance due to diminished suction capacity [25]. In straw-reinforced sand concrete, hot water treatment provided the most balanced improvement (a 30 % increase in flexural strength), while gasoil minimized shrinkage and waste oil adversely affected dimensional stability despite strength gains [26].

While various treatments have been evaluated for different plant fibers, research on prickly pear fibers remains limited, with existing studies primarily focused on hot-water treatments and assessments restricted to 28 days of age. The present study aims to fill this gap by evaluating the impact of three coating-based treatments – resin, lime solution, and bitumen – on the mechanical (compressive and flexural), physical (density), and thermal (conductivity) behavior of prickly pear fiber-reinforced concrete. The analysis extends to 180 days to evaluate the evolution of properties beyond standard curing ages. Treated and untreated composites are compared to identify the most effective method for enhancing interfacial stability and mitigating alkaline-induced degradation.

2. Materials and Methods

The development of sustainable construction materials often involves either the optimization of the binder [27] or the reinforcement of the matrix with agricultural residues [28]. In the present study, the focus is placed on the incorporation of cactus fiber sheets as a natural reinforcement within a standardized concrete matrix. All materials and experimental procedures followed the international standards prevailing in the region of study to ensure technical consistency. The binder used is a Portland cement manufactured according to EN 197-1 specifications. The mechanical characterization of the concrete was performed according to the EN 12390 series, specifically EN 12390-1 for specimen geometry (16×32 cm cylinders)

and EN 12390-6 for splitting tensile strength. The following subsections describe the aggregate and binder properties, the fiber treatments, the concrete mix design, and the experimental techniques applied.

2.1. Aggregate and Binder Properties

The binder is a CEM I 42.5 Portland cement, with a density of 3.15 g/cm^3, a compactness of 0.574, and a Blaine specific surface area of 346.6 m^2/kg. The fine aggregate is a 0/2 mm sand extracted from the Borj Hfaiedh quarry. Its measured sand equivalent (SE = 81, NF P18-597) confirms a high level of cleanliness. The coarse aggregate is a 4/12 mm gravel obtained from the Jbel Ressas quarry. The sand exhibits an apparent density of 1650 kg/m^3 and an absolute density of 2510 kg/m^3, while the gravel presents an apparent density of 1560 kg/m^3 and an absolute density of 2521 kg/m^3. The particle size distributions of the aggregates (Fig. 1) were determined by dry sieving, a methodology consistent with the characterization of alternative and conventional granular materials [29, 30]. According to EN 12620, the sand is classified by its fineness modulus, which was calculated as 1.85, identifying it as a fine sand. The coarse aggregate is classified as a 4/12 mm class gravel, with a maximum particle size $(D_{\max})$ of 12.5 mm, as confirmed by the grading analysis. These classifications are essential for ensuring an optimal granular skeleton and for monitoring the water demand of the cementitious matrix.

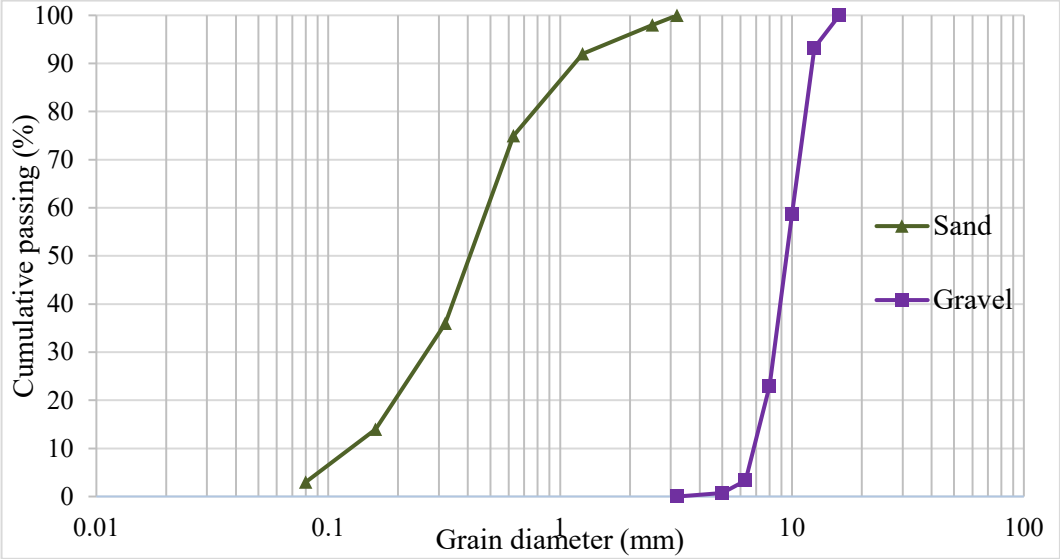

Figure 1. Particle size distribution curves for sand and gravel.

2.2. Fibers

Opuntia ficus-indica, commonly known as the prickly pear cactus, is prevalent in Africa, the Americas, and the Mediterranean basin [31]. This species is characterized by its stems, referred to as “cladodes” or “nopalitos,” which fulfill the function of leaves [32]. Upon the decay of an *Opuntia* trunk or cladode, the outer layer gradually decomposes, exposing an underlying structure composed of multiple fibrous layers arranged in a honeycomb-like pattern, as illustrated in Fig. 2.

Figure 2. Dead prickly pear cladode.

The fibers used in this study were sourced from naturally dead cladodes and trunks and manually cut into 5 × 5 cm pieces. According to Mannai et al. [33], *Opuntia ficus-indica* fibers exhibit a chemical

composition of approximately 53.6 % cellulose, 4.8 % lignin, and 10.9 % hemicellulose. While the relatively high cellulose content is favorable for mechanical performance, the presence of lignin and hemicellulose – components known to be chemically unstable in highly alkaline environments such as Portland cement – raises concerns regarding potential degradation over time when the fibers are embedded in cementitious matrices. This consideration motivates the use of protective surface treatments aimed at improving their durability within concrete. In addition to their chemical characteristics, the mechanical behavior of *Opuntia* fibers displays significant variability in the literature, as highlighted in [34]. This dispersion is mainly attributed to differences in extraction methods, environmental factors, and particularly the maturity of the cladodes. Reported tensile elastic modulus values range from 0.15 to 2.93 GPa, while tensile strengths vary between 1 and 27 MPa, with the highest values generally obtained from older cladodes where the lignocellulosic network is more developed.

The treatments applied in this study involved coating the fibers with lime, epoxy, or bitumen, as illustrated in Fig. 3. Consequently, the study examined five distinct types of concrete: ordinary concrete (OC) serving as the control; concrete reinforced with untreated prickly pear fibers (UTFC); and concretes reinforced with lime-treated (LFC), epoxy-treated (EFC), and bitumen-treated (BFC) prickly pear fibers. The lime treatment involved immersing the fibers in a lime solution for 30 seconds, followed by drying for 24 hours. This process aims to improve the bond between the fibers and the cementitious matrix. The bitumen treatment entailed immersing the fibers in bitumen heated to 160 °C, followed by drying at ambient temperature to allow the bitumen to solidify. The epoxy treatment involved coating the fibers with an epoxy resin, which acts as a binding agent that encapsulates the fibers. The objective of the bitumen and epoxy treatments is mainly to enhance the moisture protection of the fibers and, consequently, to improve their resistance to the alkaline environment.

a **b** **c** **d**

Figure 3. Untreated (a), epoxy (b), bitumen (c), and lime (d) treated fibers.

The densities of the concrete samples incorporating prickly pear fibers varied depending on the treatment applied. The untreated fibers had a density of 571 kg/m^3. While fiber density increased slightly with treatment, the maximum increase remained below 5 %. Consequently, the density variation of the fibers was neglected in the concrete mix design.

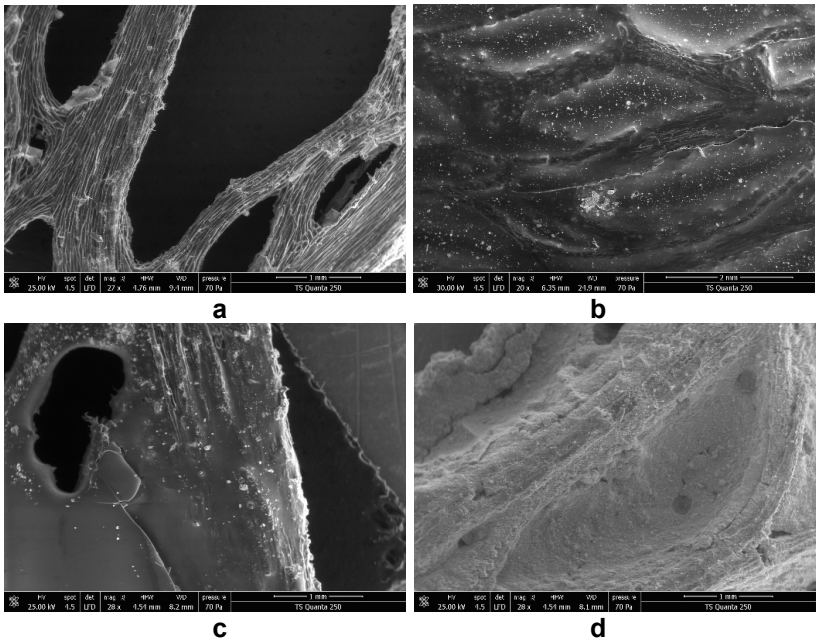

a **b**

c **d**

Figure 4. SEM of untreated (a), epoxy (b), bitumen (c), and lime (d) treated fibers.

Fig. 4 presents Scanning Electron Microscopy (SEM) images of both treated and untreated prickly pear fibers. The SEM image of the untreated fiber reveals a fibrous structure with loosely attached impurities and plant residues. In the case of the lime-treated fiber, a thin layer of lime is visible, coating the fibers and filling the gaps between them, resulting in a granular surface texture. The bitumen-treated fiber appears coated with a smooth, continuous layer of bitumen that obscures the natural surface features. The SEM image of the epoxy-treated fiber shows a uniform, smooth epoxy resin coating that encapsulates the fibers, effectively covering the natural surface texture and filling the inter-fiber spaces, with fewer visible microfibrils.

2.3. Elaboration of the Concrete

The baseline formulation (C0) was designed using the Dreux–Gorisse method to achieve a specific target consistency and strength class. The mix proportions, which resulted in a constant water-to-cement (W/C) ratio of 0.4375, are detailed in Table 1. The fibers were incorporated as a volumetric replacement for the aggregates, maintaining a constant sand-to-gravel volume ratio. Any variation in fiber density resulting from the different treatments was considered negligible and was therefore not accounted for during the mix design process. Consequently, five different fiber dosages were evaluated: 5, 10, 15, 20, and 40 kg/m^3 (Table 1).

Table 1. Composition of concrete (kg/m^3).

Designation	C0	C5	C10	C15	C20	C40
Gravel	1175	1161	1146	1132	1118	1060
Sand	646	638	630	622	613	581
Cement	400	400	400	400	400	400
Water	175	175	175	175	175	175
Fibers	0	5	10	15	20	40

The untreated and lime-treated fibers were pre-saturated with water before mixing to prevent them from absorbing water from the fresh concrete. This step was unnecessary for the epoxy- and bitumen-treated fibers, as their treatment effectively prevents water absorption. Following the mixing process, which ensured a random distribution of the fibers, three specimens of each concrete composition were prepared for each test. The specimens were demolded 24 hours after casting.

2.4. Experimental Techniques

The workability of fresh concrete was assessed using the slump test, in accordance with the aforementioned EN 12350-2. Compressive and flexural tests were performed on cubic (15 × 15 × 15 cm) and prismatic (7 × 7 × 28 cm) specimens, respectively, using a universal testing machine (Fig. 5). As previously specified, splitting tensile strength was determined on the 16 × 32 cm cylindrical specimens. These tests were performed at curing ages of 3, 7, 28, 90, and 180 days to assess the strength evolution of the concrete over time.

a **b** **c**

Figure 5. Experimental setup for compression (a), flexural (b), and splitting tensile (c).

Thermal conductivity, diffusivity, and specific heat were measured using a Fox 314 calorimeter, following the ASTM C518 and ISO 8301 standards.

3. Results and Discussion

3.1. Workability and Densities

Fig. 6 presents the effect of fiber type and treatment on the workability of the concrete. The reference OC exhibits a slump of 11.0 cm. At a low dosage of 5 kg/m^3, untreated fibers slightly reduce the slump to 10.8 cm, while bitumen-, lime-, and epoxy-treated fibers result in values of 11.1, 11.2, and 10.9 cm, respectively. These variations indicate that fiber treatments modify the fresh behavior of the mix, likely due to differences in fiber morphology and the quality of the fiber–matrix interface induced by each treatment.

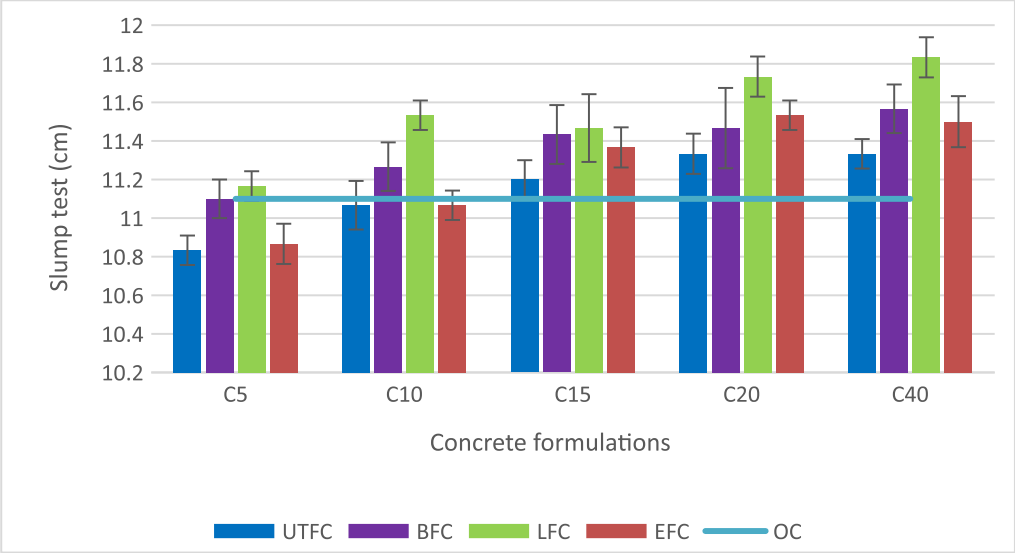

Figure 6. Workability of concrete.

As the fiber content increases, an overall improvement in workability is observed. At 40 kg/m^3, slump values reach 11.3 cm for UTFC, 11.6 cm for BFC, 11.8 cm for LFC, and 11.5 cm for EFC, confirming that the lime treatment provides the greatest enhancement, followed by bitumen and epoxy, while untreated fibers remain the least effective. Despite these changes, all mixtures maintain an S3 consistency class, indicating that the addition of treated or untreated fibers does not compromise the required workability level.

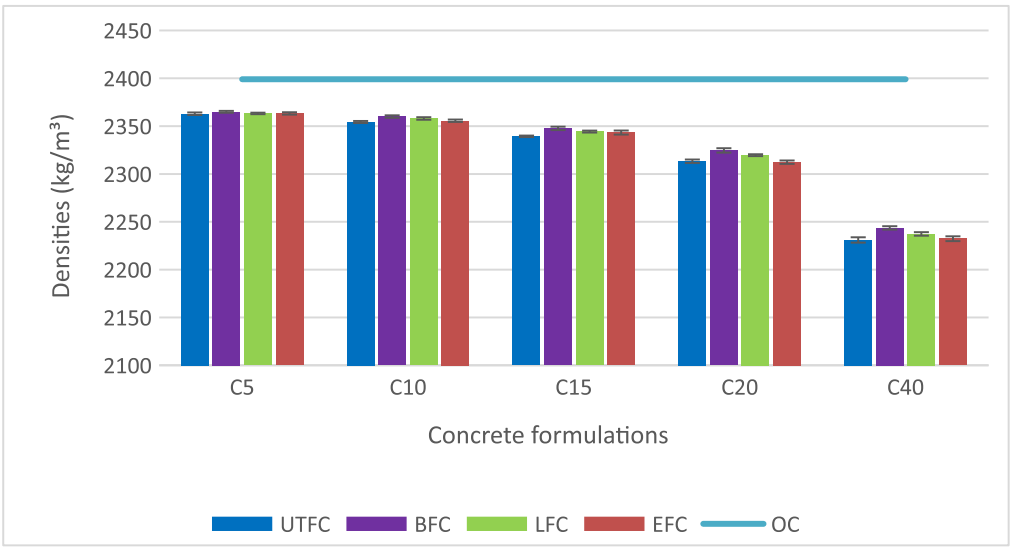

Figure 7. Density of concrete.

Fig. 7 shows that the incorporation of plant fibers leads to a measurable decrease in concrete density. The reference concrete exhibits a density of 2399 kg/m^3. At a low dosage of 5 kg/m^3, the density decreases slightly, reaching 2363–2365 kg/m^3 depending on the fiber treatment, which corresponds to a reduction of about 1.5 %. Increasing the fiber dosage amplifies this effect: at 40 kg/m^3, densities range from 2231 to 2244 kg/m^3, representing a reduction of approximately 7 % compared to the reference mix. This decrease

is primarily attributed to the partial replacement of dense mineral aggregates with fibers of significantly lower density.

3.2. Compressive Strength

Fig. 8 presents the evolution of compressive strength at 3, 7, 28, 90, and 180 days for the different concrete formulations. The reference concrete exhibits strengths of 36.3 MPa at 28 days, increasing to 37.5 MPa at 90 days and 38.5 MPa at 180 days, reflecting the expected hydration of the cement matrix over time.

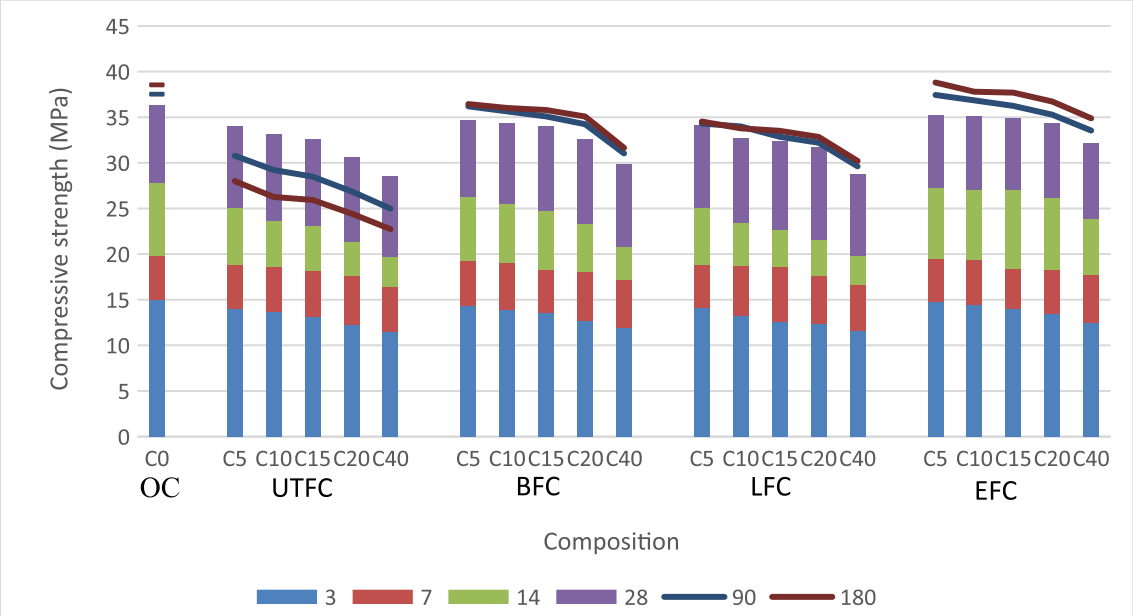

Figure 8. Compressive strength at different ages (S_{dmax} = 0.8 MPa).

For all fiber dosages and treatments, the incorporation of plant fibers leads to a reduction in compressive strength compared to the reference mix. At low dosages, this reduction remains limited, but it becomes more pronounced at higher fiber contents. At a dosage of 40 kg/m^3, UTFC exhibits a 28-day strength of 28.5 MPa, corresponding to a reduction of approximately 21.5 % relative to OC. The effect of fiber treatment is clearly observable: LFC reaches 28.8 MPa (a ≈ 20 % reduction), BFC reaches 29.8 MPa (a ≈ 17 % reduction), while EFC achieves the highest value, 32.2 MPa, representing only an 11 % strength loss at 28 days. These results confirm that surface conditioning of the fibers mitigates the mechanical performance loss caused by fiber addition.

Strength evolution over time further highlights the contrasting behavior between untreated and treated fibers. For UTFC at 40 kg/m^3, strength continues to decrease beyond 28 days, reaching 25.0 MPa at 90 days and 22.7 MPa at 180 days, corresponding to reductions of 33 and 41 % relative to OC. This progressive deterioration suggests fiber degradation within the alkaline cementitious environment. In contrast, concretes incorporating treated fibers exhibit strength gains between 28 and 180 days, similar to the trend observed in OC. At 90 and 180 days, reductions relative to the reference mix range from 21 % for LFC to 17–18 % for BFC and only 9.5–10.5 % for EFC. The long-term improvement observed for treated mixes confirms that fiber treatments enhance durability and stabilize fiber–matrix interactions, preventing the degradation observed in untreated fibers.

The microstructural observations obtained through optical microscopy (Fig. 9) reinforce the mechanical results by illustrating the distinct behaviors of treated and untreated fibers within the cementitious matrix. In specimens containing untreated fibers, several degradation features are apparent. Figs. 9d to 9f show interfacial gaps and fiber–matrix detachment, indicating insufficient adhesion and early debonding. Adjacent voids and the altered morphology of the fibers provide evidence of moisture-driven swelling and subsequent shrinkage, mechanisms known to promote fiber–matrix debonding, as documented in several studies [35–38]. In Fig. 9g, the fiber appears partially cracked and separated from the surrounding matrix, while Fig. 9h shows a longitudinal subdivision of the fiber into individual microfilaments located within a void. Notably, matrix cracking is not observed in these regions, confirming that degradation primarily affects the fibers and their interface rather than the cement paste itself. These mechanisms explain the progressive loss of mechanical performance observed between 28 and 180 days.

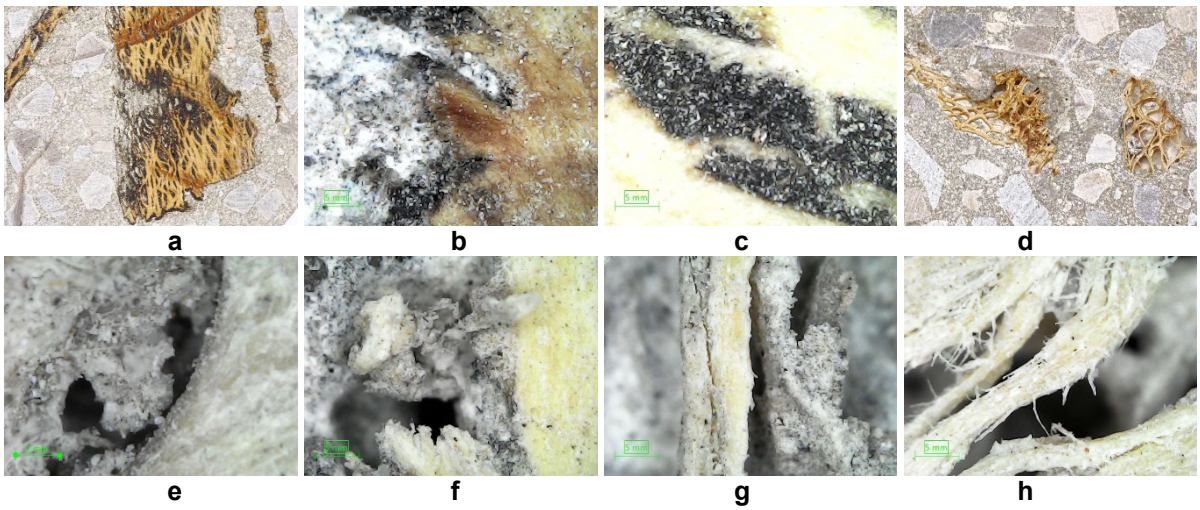

Figure 9. An image of concrete with fibers treated by bitumen (a), microscopic images fibers treated by bitumen in concrete (b, c), an image of concrete with untreated fibers (d), microscopic images of untreated fibers in concrete (e–h).

In contrast, treated fibers exhibit markedly improved interfacial behavior. Figs. 9a to 9c show continuous, well-bonded interfaces without visible detachment or voids. The protective coating limits water ingress and reduces direct exposure to the alkaline pore solution, thereby preventing swelling-induced stresses and preserving interfacial integrity. These stabilized fiber–matrix interactions directly correlate with the improved and sustained compressive strength development observed beyond 28 days in concretes incorporating treated fibers.

3.3. Flexural Strength

The flexural strength results at 3, 7, 28, 90, and 180 days for all mixtures and fiber treatments are presented in Fig. 10. The reference concrete (C0) exhibits a flexural strength of 2.8 MPa at 28 days, increasing slightly to 2.85 MPa at 90 days and 2.92 MPa at 180 days. The introduction of plant fibers significantly improves flexural performance, with the magnitude of enhancement depending on fiber dosage and treatment.

At the lowest dosage (C5), the 28-day flexural strength increases to 7.9–9.7 MPa depending on the treatment, which corresponds to improvements of approximately 180 to 245 % relative to C0. In this case, lime treatment yields the lowest strength values – slightly higher than those of untreated fibers – whereas bitumen and epoxy treatments achieve considerably greater gains. The C15 mixtures exhibit the highest flexural strengths across all curing ages, with 28-day values ranging from 9.2 MPa for lime-treated fibers to 12.1 MPa for epoxy-treated fibers, representing increases of approximately 229 to 333 % relative to the C0. This dosage consistently maximizes the efficiency of fiber incorporation, irrespective of the treatment applied.

At the highest dosage (C40), flexural strengths at 28 days remain markedly higher than those of the C0, with values of 7.6 MPa for untreated fibers, 7.7 MPa for lime treatment, 8.2 MPa for bitumen treatment, and 10.7 MPa for epoxy treatment. Although these absolute values are slightly lower than those at C15, the same hierarchy among treatments is observed, with epoxy remaining the most effective and lime providing the lowest improvement.

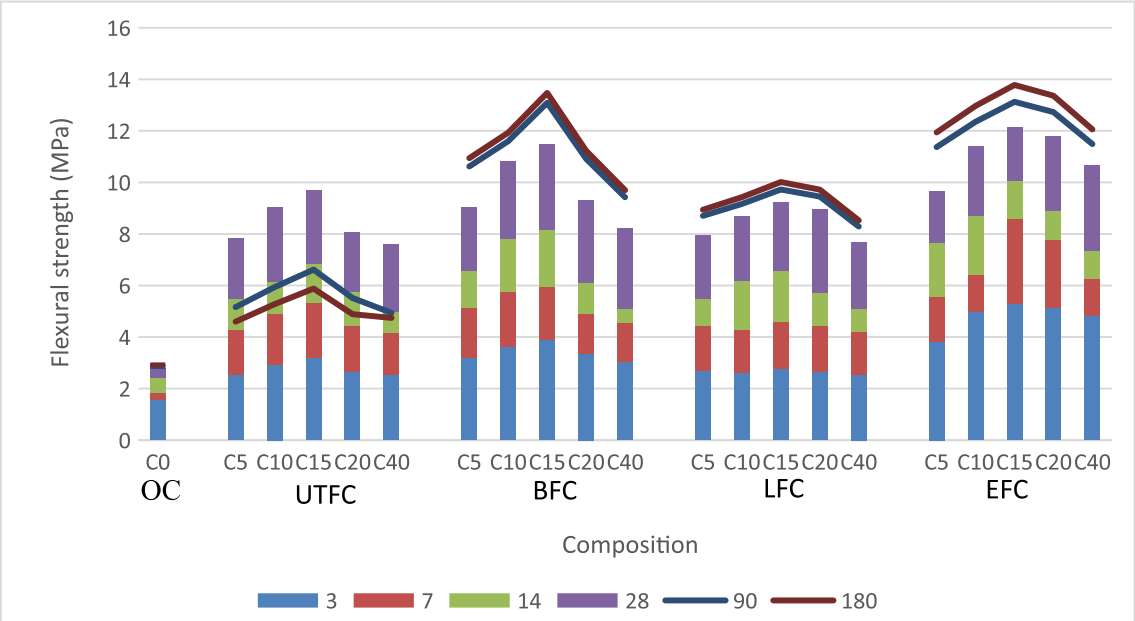

Figure 10. Flexural strength results (S_{dmax} = 0.45 MPa).

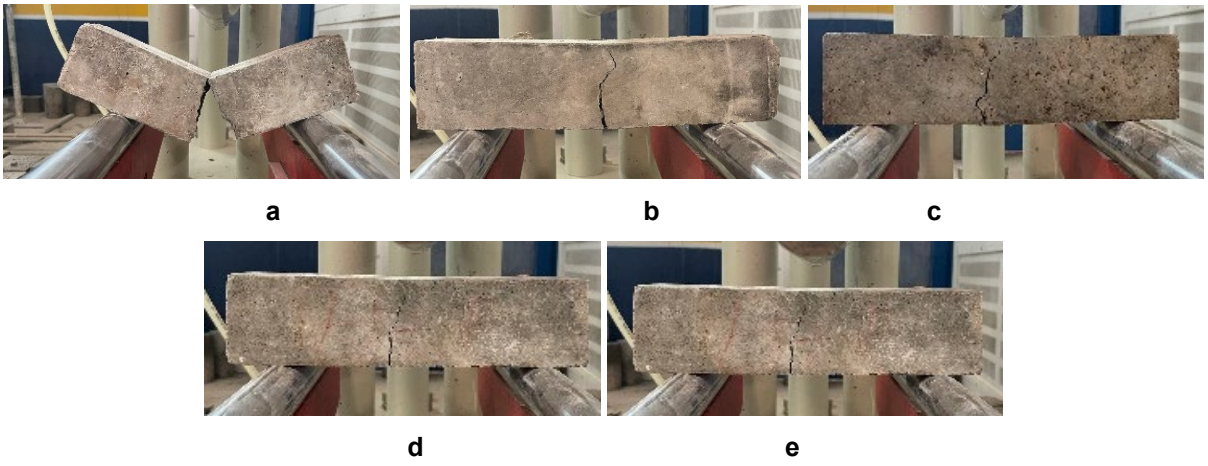

Figure 11. Flexural test: a – OC, b – UTFC, c – BFC, d – LFC, e – EFC.

Post-failure observations presented in Fig. 11 further support these results. The C0 exhibits brittle fracture and complete separation once the maximum load is reached, which is characteristic of unreinforced cementitious materials. In contrast, fiber-reinforced specimens retain partial integrity after failure due to fibers bridging the cracked surfaces and maintaining residual load transfer. This bridging mechanism, widely reported in the literature for cementitious composites incorporating natural fibers [5, 17], explains the substantial increase in flexural strength observed despite the reduction in compressive strength.

Fig. 12 shows SEM images of crack zones in specimens incorporating bitumen-treated fibers. The images reveal fibers fully coated with bitumen and embedded within a continuous and cohesive interface, with no visible separation between the coating and the surrounding cement matrix. These results are consistent with the optical microscopy observations (Fig. 9) and confirm that the protective coating stabilizes the fiber–matrix interface, enhances stress transfer after matrix cracking, and contributes to the sustained flexural performance for up to 180 days.

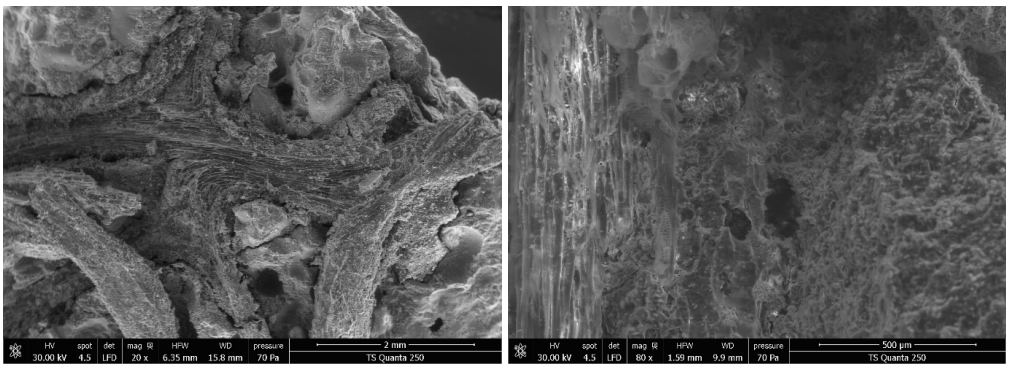

a b

Figure 12. SEM of concrete with fibers treated by bitumen: a – concrete and fibers, b – concrete and fiber interface.

The evolution of the flexural strength relative to the compressive strength provides further insight into the mechanical behavior of the fiber-reinforced concrete. According to Ahmed et al. [39], the relationship between the flexural tensile strength f_R and the compressive strength f_c is frequently expressed in the literature as a power equation in the form $f_R = af_c^n$. Several standards provide formulas for this relationship in the form $f_R = af_c^{0.5}$. For instance, AS 3600 and CSA-A23.3 specify $f_R = 0.6f_c^{0.5}$, while the ACI 363-92 standard proposes a different equation: $f_R = 0.94f_c^{0.5}$ [40]. Fig. 13 presents the flexural tensile strength as a function of the compressive strength for the current study.

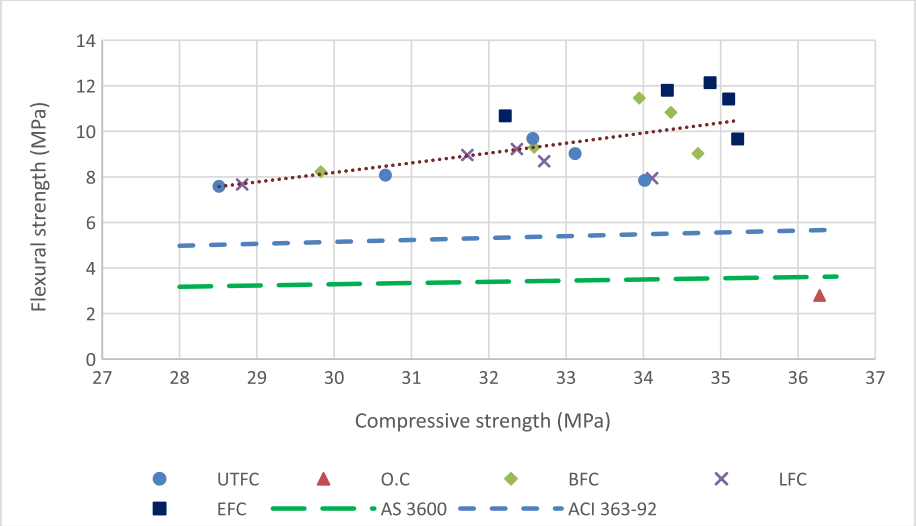

Figure 13. Flexural and compressive strength relationship.

The experimental results exhibit a clear increasing trend of flexural strength relative to compressive strength. A power-law regression performed on the experimental dataset of the fibrous concrete specimens (treated and untreated) yielded the following relationship:

$$f_R = 0.045f_c^{1.533}. \quad (1)$$

The exponent obtained from this regression (1.533) is significantly higher than the value implicitly assumed in current design standards (0.5), indicating that the flexural strength of fibrous concrete increases at a faster rate than predicted by code-based formulations. This behavior reflects the dominant role of the reinforcement and matrix modification mechanisms under flexural loading.

Fig. 13 further shows that the fibrous concrete specimens subjected to epoxy and bitumen treatments are located in the upper-right region of the diagram, corresponding to the highest flexural and compressive strength values. This indicates that these two treatments are the most effective in enhancing overall mechanical performance, particularly in flexure. This superior behavior can be attributed to the improved crack-bridging efficiency of the fibers, combined with enhanced fiber–matrix interaction and reduced

microcrack propagation due to the presence of epoxy or bitumen. By contrast, the non-fibrous concrete is represented by a single data point located in the lower region of the figure, lying very close to the AS 3600 prediction curve. This observation confirms that, in the absence of fiber reinforcement, the standard code-based relationship remains applicable within the investigated strength range.

Overall, the deviation of the fibrous and treated concretes from the normative predictions highlights the limitations of existing flexural–compressive strength relationships when applied to modified concretes. The proposed empirical relationship should therefore be interpreted as representative of fibrous concrete behavior within the investigated domain, with epoxy and bitumen treatments playing a key role in achieving superior flexural performance.

3.4. Splitting Tensile Strength

Fig. 14 shows the evolution of the splitting tensile strength. The values at 28, 90, and 180 days – points at which mechanical properties stabilize – allow for a direct comparison. The C0 records 2.18, 2.22, and 2.27 MPa at these ages. Incorporating fibers significantly enhances tensile performance, with the maximum improvement obtained at a dosage of 15 kg/m^3. At 28 days, C15 exhibits tensile strengths of 7.84 MPa with untreated fibers, 7.47 MPa with lime-treated fibers, 9.28 MPa with bitumen-treated fibers, and 9.82 MPa with epoxy-treated fibers. These values correspond to increases of approximately 260, 243, 326, and 350 % relative to the C0. At later ages, untreated fibers show a decline in tensile strength (5.45 MPa at 90 days and 4.68 MPa at 180 days), whereas lime-, bitumen-, and epoxy-treated fibers maintain or improve their performance, reaching up to 11.17 MPa at 180 days with epoxy treatment. Increasing the fiber dosage to 40 kg/m^3 reduces tensile strength relative to C15 but still yields values higher than those of the C0. At 28 days, C40 reaches 6.14 MPa for untreated fibers, 6.21 MPa for lime-treated fibers, 6.69 MPa for bitumen-treated fibers, and 8.64 MPa for epoxy-treated fibers. This confirms that excessive fiber content induces fiber clustering and matrix discontinuities, limiting mechanical efficiency [41].

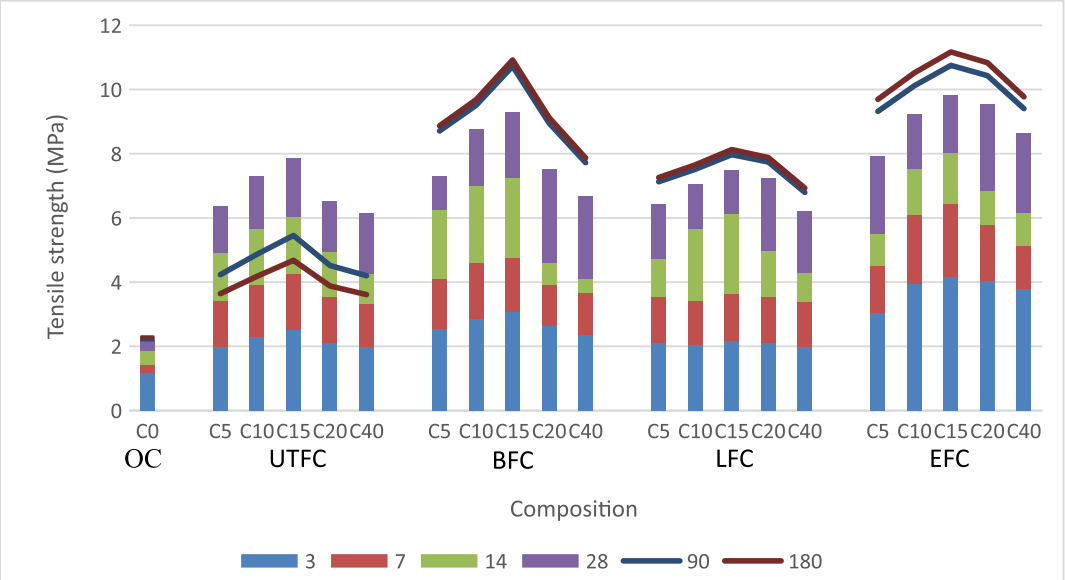

Figure 14. Splitting tensile test results.

The failure patterns support the mechanical observations. The C0 splits abruptly into two detached halves, whereas the fiber-reinforced specimens remain connected after testing, with the cracks bridged by fibers. Manual separation reveals fracture surfaces containing randomly distributed prickly pear fibers (Fig. 15), most of which underwent fracture rather than pullout. This indicates strong fiber–matrix adhesion, particularly in the treated-fiber mixtures.

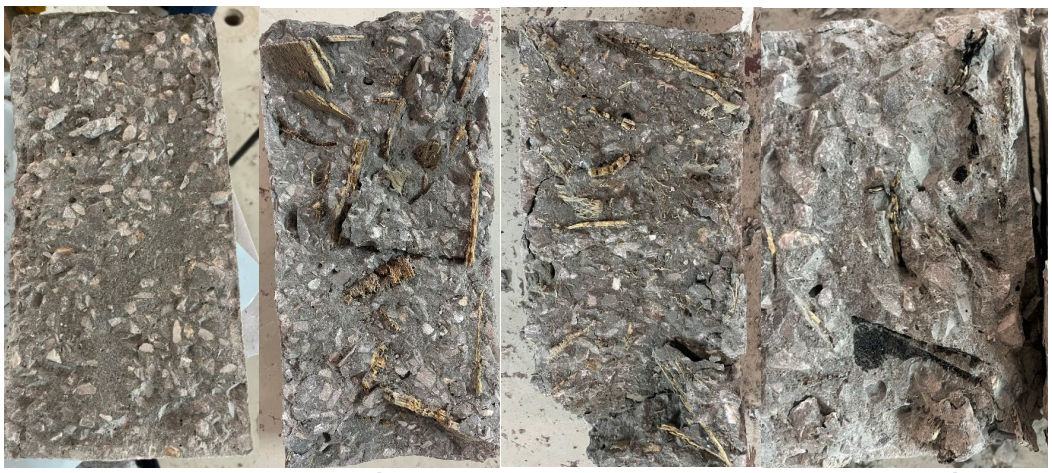

a b c d

Figure 15. Splitting tensile test results: a – OC, b – EFC, c – LFC, d – BFC.

3.5. Thermal Characteristics

This section examines the influence of prickly pear fibers and their surface treatments on the thermal behavior of concrete. Three fundamental properties are considered: thermal conductivity, specific heat capacity, and thermal diffusivity. These parameters are intrinsically linked to the microstructure of cementitious composites and are affected by the addition of low-conductivity plant fibers.

3.5.1. Thermal conductivity

Thermal conductivity governs the heat transfer capacity of cementitious composites and is strongly influenced by microstructural variables such as moisture content, aggregate volume fraction, pore connectivity, and the nature of the embedded inclusions. Fig. 16 reports the evolution of thermal conductivity as a function of fiber dosage and surface treatment. A monotonic reduction is observed with increasing fiber content, with values decreasing from 1.91 W/(m·K) for the reference mixture to a range of 1.04–1.14 W/(m·K) at 40 kg/m^3, depending on the treatment; this corresponds to a decrease of approximately 40–45 %. Given that common mineral aggregates exhibit conductivities between 1.16 and 8.6 W/(m·K) [42], such reductions are consistent with the replacement of higher-conductivity constituents with materials of lower intrinsic conductivity.

The decrease in effective conductivity can be explained by considering the microstructural role of the fibers. Materials with low intrinsic conductivity or highly porous internal structures act as insulating inclusions that alter the topology of conduction pathways. With an intrinsic conductivity of approximately 0.057 W/(m·K) and a naturally porous morphology, prickly pear fibers reduce the continuity of solid heat transfer routes within the matrix and, therefore, behave as thermally insulating inclusions.

To assess these experimental results, they were compared with classical homogenization models formulated for isotropic two-phase composites. The cementitious matrix is considered the continuous phase with conductivity λ_m, while the prickly pear fibers constitute the dispersed phase with conductivity λ_f, and respective volume fractions V_m and V_f satisfying $V_m + V_f = 1.$ Under these assumptions, the extremal estimates of effective conductivity are provided by the Voigt and Reuss bounds [43]:

$$\lambda_V = V_m \lambda_m + V_f \lambda_f; \tag{2}$$

$$\lambda_R = \left(\frac{V_m}{\lambda_m} + \frac{V_f}{\lambda_f} \right)^{-1}. \tag{3}$$

Eqs. (2) and (3) represent the maximal conductivity corresponding to a parallel-phase configuration and the minimal conductivity associated with a series configuration, respectively. Although these idealized morphologies are not strictly representative of the present composite, they provide an essential admissible interval for assessing the effective thermal behavior. A more physically constrained prediction is given by the Hashin–Shtrikman bounds, which are derived from variational principles and are applicable to isotropic composites with arbitrarily shaped inclusions [44]:

$$\lambda_{HS+} = \lambda_m + \frac{V_f}{\frac{1}{\lambda_f - \lambda_m} + \frac{V_m}{3\lambda_m}}; \tag{4}$$

$$\lambda_{HS-} = \lambda_f + \frac{V_m}{\frac{1}{\lambda_m - \lambda_f} + \frac{V_f}{3\lambda_f}}. \tag{5}$$

These bounds (Eqs. (4) and (5)) define the narrowest theoretically admissible interval for the effective conductivity of an isotropic two-phase material. The measured values remain well below the Voigt limit while staying above the Reuss bound; however, in several cases, they lie below the Hashin–Shtrikman lower limit. This departure indicates that the actual microstructure – featuring elongated pores, anisotropic fiber arrangements, and potentially a third interfacial phase – creates a higher thermal tortuosity than assumed in classical isotropic models.

The slightly higher conductivities measured for the treated fibers are consistent with improved interfacial bonding. Enhanced adhesion reduces the volume of interfacial air voids – the conductivity of which is extremely low – increasing the continuity of solid heat transfer paths and, consequently, raising the effective thermal conductivity.

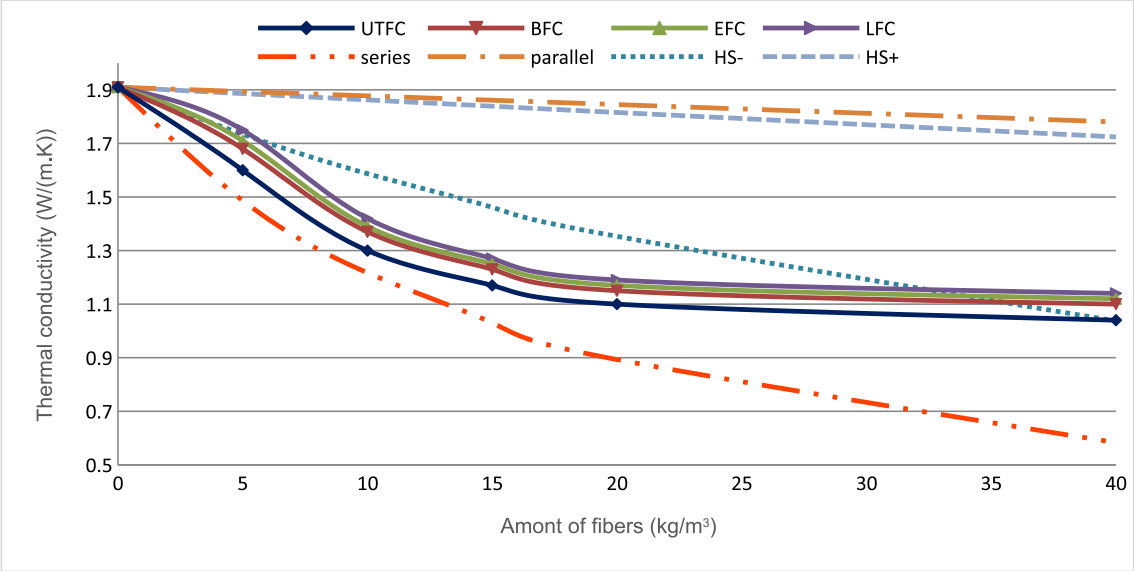

Figure 16. Thermal conductivity of concrete incorporating treated fibers (S_{dmax} = 0.015 W/(m.K)).

3.5.2. Specific heat

Specific heat capacity (c_p) represents the amount of heat required to increase the temperature of a unit mass by one degree [40]. In cementitious materials, this property depends on the thermal behavior of the constituent solid phases. Prickly pear fibers contain high fractions of cellulose, hemicellulose, and lignin, which exhibit greater heat capacities than mineral aggregates. Their cellular microstructure, rich in voids and capable of retaining bound water, also contributes to increasing the heat storage capacity of the composite.

Fig. 17 shows that the incorporation of fibers leads to a systematic increase in the specific heat capacity for all treatment types. When considering only the reinforced mixtures (5–40 kg/m^3), the evolution of c_p with fiber dosage is quasi-linear. This behavior is consistent with a progressive increase in the volumetric fraction of organic phases, whose intrinsic heat capacity is significantly higher than that of the mineral matrix. At 40 kg/m^3, the specific heat capacity rises by approximately 22–24 % compared to the C0.

Differences between treatment types follow a consistent hierarchy across all dosages. EFC systematically exhibits the highest c_p values, with an increase of approximately 1–3 % relative to UTFC. This enhancement is primarily linked to the stabilization of the fiber surface by the epoxy coating, which

prevents fiber degradation and preserves a durable and continuous contact with the cement matrix. LFC shows slightly lower values, typically within 0.5–2 % lower than those of EFC, reflecting the partial mineralization induced by the lime treatment and the improved compatibility of the fibers with the surrounding matrix. UTFC presents the lowest c_p values among the reinforced mixtures. This is attributed to the absence of surface modification, which results in weaker fiber–matrix adhesion and a less efficient contribution of the fibers to the overall thermal storage capacity. Collectively, the results indicate that both fiber dosage and surface treatment contribute to variations in the specific heat capacity of the composite, with the dominant effect being associated with the fiber fraction.

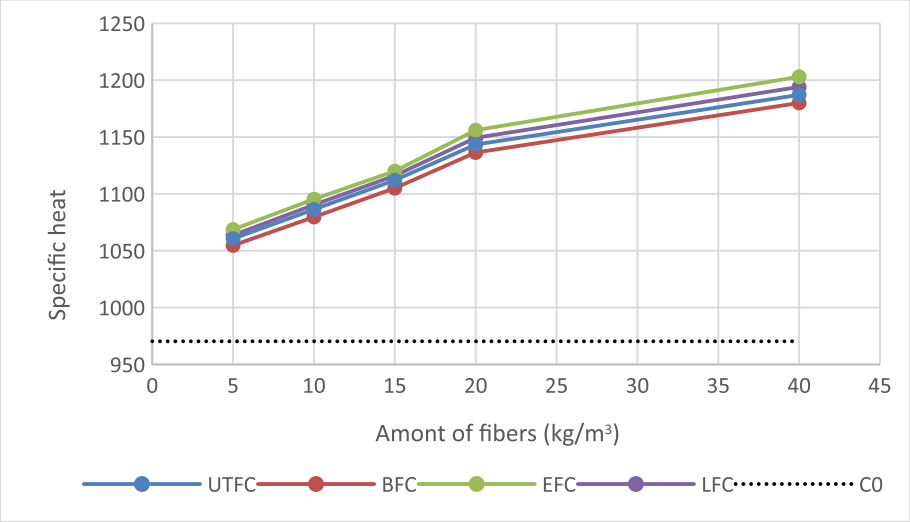

Figure 17. Specific heat of concrete incorporating treated fibers (S_{dmax} = 4.5 J/(kg.K)).

3.5.3. Thermal diffusivity

Thermal diffusivity α quantifies the rate at which heat propagates through a material and is defined as:

$$a = \frac{\lambda}{\rho c_p}\left(\mathrm{m}^2/\mathrm{s}\right), \tag{6}$$

where λ represents the thermal conductivity (W/(m.K)), ρ is the density (kg/m³), and c_p is the specific heat capacity (J/(kg·K)).

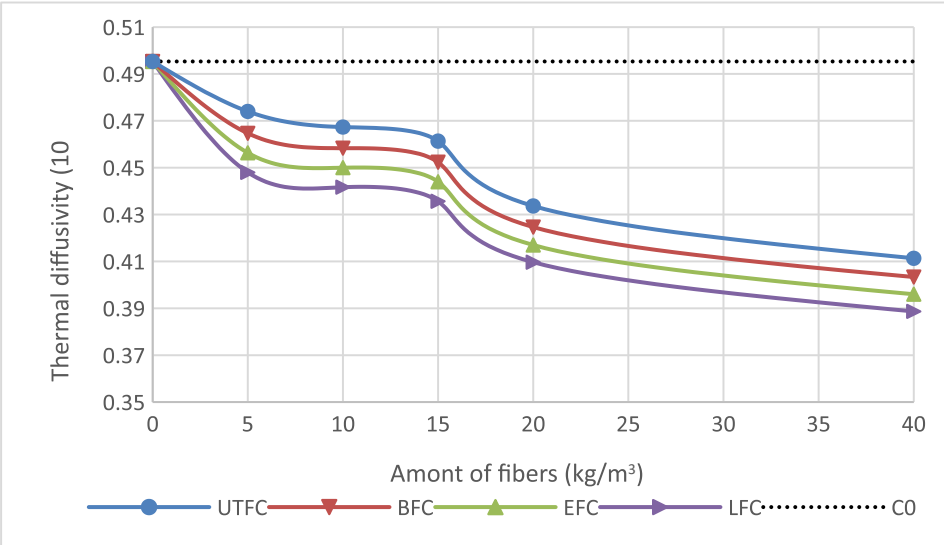

Figure 18. Thermal diffusivity of concrete incorporating treated fibers (S_{dmax} = 4×10^{-9} m^2/s).

Fig. 18 shows that thermal diffusivity decreases consistently with increasing fiber content, regardless of the treatment applied. The C0 presents a diffusivity of 0.50 mm²/s. At 40 kg/m³, the values decrease to

0.41 mm²/s for UTFC, 0.40 mm²/s for BFC, 0.40 mm²/s for EFC, and 0.39 mm²/s for LFC, representing reductions of approximately 18–22 %.

This reduction stems primarily from microstructural modifications induced by the fibers and their treatments. The dominant factor is the marked decrease in thermal conductivity λ: the fibers and their internal air cavities lower the effective conductivity of the composite by about 40–45 % at 40 kg/m³, directly reducing the numerator of α. A secondary effect arises from changes in the volumetric heat capacity ρc_p: fiber incorporation increases c_p by roughly 22–24 % while slightly reducing the bulk density (≈7 %), which increases the denominator of α and contributes further to the decrease in diffusivity. Although the reduction in density alone would tend to raise α, the combined effect of reduced conductivity and increased heat capacity overrides this tendency, producing the observed decline.

Differences among treatments remain limited but systematic. Epoxy- and bitumen-treated fibers lead to the lowest diffusivities at equivalent dosages, followed by lime-treated fibers, which slightly outperform untreated ones at higher fiber contents. These distinctions reflect the influence of surface treatments on fiber integrity and interfacial contact: epoxy and bitumen create more stable coatings that limit interfacial voids and maintain the insulating character of the fibers, whereas lime treatment induces partial mineralization that modifies thermal behavior to a lesser extent. The overall decrease in diffusivity shows that the presence of prickly pear fibers enhances the material's thermal inertia by simultaneously restricting heat transfer and increasing its heat storage capacity.

4. Conclusion

This study investigated the long-term mechanical and thermal performance of concrete reinforced with prickly pear fibers, comparing untreated fibers with three coatings: epoxy, bitumen, and lime. The following findings highlight the main contributions of this research:

1. Surface conditioning of the fibers significantly mitigates the loss of compressive strength; notably, the epoxy treatment limits the 28-day reduction to only 11 %, compared to a 21.5 % loss for untreated fibers at a dosage of 40 kg/m³.
2. Long-term durability is critically enhanced by these treatments. While untreated fibers degrade in the alkaline cementitious environment (reaching a 41 % strength loss at 180 days), treated fibers maintain stable performance, with strength reductions relative to the reference mix limited to 10.5–21 % at the same age.
3. An optimal dosage of 15 kg/m³ maximizes mechanical efficiency, yielding peak increases in flexural and splitting tensile strengths at 28 days of up to 333 and 350 %, respectively (obtained with epoxy-treated fibers).
4. High fiber content (40 kg/m³) leads to a relative decline in mechanical performance compared to the 15 kg/m³ dosage due to fiber clustering and matrix discontinuities; however, values remain significantly higher than those of the plain reference concrete (0 kg/m³) in both flexural and tensile strength.
5. Thermal properties are substantially improved with increasing fiber content. A dosage of 40 kg/m³ achieves a 40–45 % reduction in thermal conductivity and a 22–24 % increase in specific heat capacity. This enhancement is driven by the higher volumetric fraction of organic phases, with epoxy-treated concrete showing the highest thermal storage capacity due to stabilized fiber-matrix adhesion.

In summary, pretreating prickly pear fibers – particularly with epoxy – overcomes the durability limitations typically associated with natural fibers, offering a high-performance, sustainable alternative with reliable long-term properties.

References

1. Rachedi, M., Kriker, A. Thermal Properties of Plaster Reinforced with Date Palm Fibers. Civil and Environmental Engineering. 2020. 16(2). Pp. 259–266. DOI: 10.2478/cee-2020-0025
2. Özkılıç, Y.O., Beskopylny, A.N., Stel'makh, S.A., Shcherban, E.M., Mailyan, L.R., Meskhi, B., Madenci, E. Lightweight expanded-clay fiber concrete with improved characteristics reinforced with short natural fibers. Case Studies in Construction Materials. 2023. 19. Article no. e02367. DOI: 10.1016/j.cscm.2023.e02367
3. Marvila, M.T., Rocha, H.A., de Azevedo, A.R.G., Colorado, H.A., Zapata, J.F., Vieira, C.M.F. Use of natural vegetable fibers in cementitious composites: concepts and applications. Innovative Infrastructure Solutions. 2021. 6. Article no. 180. DOI: 10.1007/s41062-021-00551-8

4. Arcila Londoño, S.L., Garcia Chumacero, J.M., Villegas Granados, L.M., Damiani Lazo, C.A., Arriola Carrasco, G.G., Villena Zapata, L.I., Idrogo Perez, C.A. Valorization of treated bamboo fiber in the mechanical strength and durability of concrete. Innovative Infrastructure Solutions. 2025. 10(6). Article no. 219. DOI: 10.1007/s41062-025-02022-w
5. Kammoun, Z., Trabelsi, A. A high-strength lightweight concrete made using straw. Magazine of Concrete Research. 2020. 72(9). Pp. 460–470. DOI: 10.1680/jmacr.19.00225
6. Lahouioui, M., Ben Arfi, R., Fois, M., Ibos, L., Ghorbal, A. Investigation of Fiber Surface Treatment Effect on Thermal, Mechanical and Acoustical Properties of Date Palm Fiber-Reinforced Cementitious Composites. Waste and Biomass Valorization. 2020. 11. Pp. 4441–4455. DOI: 10.1007/s12649-019-00745-3
7. Sonebi, M., Abdalqader, A., Amziane, S., Dvorkin, L., Ghorbel, E., Kenai, S., Khatib, J., Lushnikova, N., Perrot, A. Trends and opportunities of using local sustainable building materials in the Middle East and North Africa region. RILEM Technical Letters. 2022. 7. Pp. 127–138. DOI: 10.21809/rilemtechlett.2022.169
8. Charai, M., Mezrhab, A., Moga, L., Karkri, M. Hygrothermal, mechanical and durability assessment of vegetable concrete mixes made with Alfa fibers for structural and thermal insulating applications. Construction and Building Materials. 2022. 335. Article no. 127518. DOI: 10.1016/j.conbuildmat.2022.127518
9. Abdelouahed, A., Kechkar, C., Hebhoub, H., Merzoud, M., Enhancing the Performance and Durability of Eco-Friendly Mortar with Diss Fibers (Ampelodesmos *mauritanicus*). Revue des Composites et des Matériaux Avancés – Journal of Composite and Advanced Materials. 2023. 33(4). Pp. 219–226. DOI: 10.18280/rcma.330402
10. Ramasubramani, R., Gunasekaran, K. Study on plastic shrinkage of coconut shell concrete slab made with M-sand. Innovative Infrastructure Solutions. 2022. 7(1). Article no. 12. DOI: 10.1007/s41062-021-00614-w
11. Muñoz Pérez, S.P., Alarcón Peltroche, M., Eugenio Pachas, E.T., Villena Zapata, L.I., Bernal Izquierdo, A.P., Rodriguez Lafitte, E.D., García Chumacero, J.M. Effect of Peruvian sisal fiber on the mechanical and microstructural strength of concrete. Innovative Infrastructure Solutions. 2025. 10. Article no. 257. DOI: 10.1007/s41062-025-02061-3
12. Hasan, N.M.S., Sobuz, M.H.R., Shaurdho, N.M.N., Basit, M.A., Paul, S.C., Meraz, M.M., Miah, M.J. Investigation of Lightweight and Green Concrete Characteristics Using Coconut Shell Aggregate as a Replacement for Conventional Aggregates. International Journal of Civil Engineering. 2024. 22(1). Pp. 37–53. DOI: 10.1007/s40999-023-00881-x
13. Tahenti, B., Trabelsi, A., Kammoun, Z. Enhancing concrete's ballistic impact resistance using Alfa fiber. International Journal of Protective Structures. 2024. 16(2). Pp. 529–547. DOI: 10.1177/20414196241271452
14. Paisig Saucedo, B.Y., Muñoz Pérez, S.P., García Chumacero, J.M., Sánchez Diaz, E., Villena Zapata, L.I., Diaz Ortiz, E.A., Rodriguez Laffite, E.D., Zuloeta, O.C., Ramos Brast, C.E. Experimental and microstructural study of concrete reinforced with maguey fiber: Peruvian case. Innovative Infrastructure Solutions. 2024. 9(12). Article no. 451. DOI: 10.1007/s41062-024-01761-6
15. Ren, G., Yao, B., Huang, H., Gao, X. Influence of sisal fibers on the mechanical performance of ultra-high performance concretes. Construction and Building Materials. 2021. 286. Article no. 122958. DOI: 10.1016/j.conbuildmat.2021.122958
16. Saad, M., Agwa, I.S., Abdelsalam, B., Amin, M. Improving the brittle behavior of high strength concrete using banana and palm leaf sheath fibers. Mechanics of Advanced Materials and Structures. 2022. 29(4). Pp. 564–573. DOI: 10.1080/15376494.2020.1780352
17. Kammoun, Z., Trabelsi, A. Development of lightweight concrete using prickly pear fibres. Construction and Building Materials. 2019. 210. Pp. 269–277. DOI: 10.1016/j.conbuildmat.2019.03.167
18. Trabelsi, A., Kammoun, Z. Mechanical properties and impact resistance of a high-strength lightweight concrete incorporating prickly pear fibres. Construction and Building Materials. 2020. 262. Article no. 119972. DOI: 10.1016/j.conbuildmat.2020.119972
19. Vo, L.T., Navard, P. Treatments of plant biomass for cementitious building materials – A review. Construction and Building Materials. 2016. 121. Pp. 161–176. DOI: 10.1016/j.conbuildmat.2016.05.125
20. Santos, S.F.D., Tonoli, G.H.D., Mejia, J.E.B., Fiorelli, J., Savastano Jr, H. Non-conventional cement-based composites reinforced with vegetable fibers: A review of strategies to improve durability. Materiales de Construcción. 2015. 65(317). Article no. e041. DOI: 10.3989/mc.2015.05514
21. Traoré, Y., Messan, A., Tsobnang, F., Gérard, J. Propriétés mécaniques d'un béton de granulats légers à base de coques de noix de palme traitées. 33èmes rencontres universitaires de Génie Civil. Université de Pau et des pays de l'Adour, 2015. Pp. 27–29.
22. Sellami, A., Merzoud, M., Amziane, S. Improvement of mechanical properties of green concrete by treatment of the vegetals fibers. Construction and Building Materials. 2013. 47. Pp. 1117–1124. DOI: 10.1016/j.conbuildmat.2013.05.073
23. Hussain, T.H., Alwan, A.S., Manea, A.K., Naje, A.S., Al-Zubaidi, H.A.M. Mechanical and Microstructural Properties of Lime-Treated Palmdate Fiber Cement Composites for Sustainable Development. Journal of Green Engineering. 2021. 11(2). Pp. 1767–1777. DOI: 10.13140/RG.2.2.35215.30881
24. Bederina, M., Gotteicha, M., Belhadj, B., Dheily, R. M., Khenfer, M.M., Queneudec, M. Drying shrinkage studies of wood sand concrete – Effect of different wood treatments. Construction and Building Materials. 2012. 36. Pp. 1066–1075. DOI: 10.1016/j.conbuildmat.2012.06.010
25. Nozahic, V., Amziane, S. Influence of sunflower aggregates surface treatments on physical properties and adhesion with a mineral binder. Composites Part A: Applied Science and Manufacturing. 2012. 43(11). Pp. 1837–1849. DOI: 10.1016/j.compositesa.2012.07.011
26. Bederina, M., Belhadj, B., Ammari, M.S., Gouilleux, A., Makhloufi, Z., Montrelay, N., Quéneudéc, M. Improvement of the properties of a sand concrete containing barley straws – Treatment of the barley straws. Construction and Building Materials. 2016. 115. Pp. 464–477. DOI: 10.1016/j.conbuildmat.2016.04.065
27. Arfien Khan, M.A., Saha, M.S., Sultana, S., Mustafi, S. Possible Use of Coal Fly Ash for Portland Cement Clinker Synthesis. Iranian Journal of Science and Technology, Transactions of Civil Engineering. 2026. 50. Pp. 1531–1539. DOI: 10.1007/s40996-025-01887-2
28. Burga Bustamante, G., Muñoz Pérez, S.P., García Chumacero, J.M., Sánchez Diaz, E., Ruiz Pico, A.A., Rodriguez Laffite, E.D., Damiani Lazo, C.A., Ramos Brast, C.E. Evaluation of the mechanical behavior of concrete with the addition of dry corn fiber. Innovative Infrastructure Solutions. 2025. 10(1). Article no. 29. DOI: 10.1007/s41062-024-01839-1
29. Shen, N.J., Hasan, M. Transforming waste into stability: improving the soft clay soil with polyethylene terephthalate (PET) column as a sustainable solution. Journal of Engineering and Applied Science. 2025. 72(1). Article no. 52. DOI: 10.1186/s44147-025-00620-0

30. Shen, N.J., Hasan, M. Installation of polyethylene terephthalate (PET) columns to promote the soil-bearing capacity of soft kaolin clay. Journal of King Saud University – Engineering Sciences. 2025. 37(4). Article no. 14. DOI: 10.1007/s44444-025-00011-z
31. Sabtain, B., Farooq, R., Shafique, B., Ranjha, M., Mahmood, S., Mueen-Ud-Din, G., Irfan, S., Shehzadi, K., Rubab, Q., Asad, L., Ishfaq, M. A Narrative Review on the Phytochemistry, Nutritional Profile and Properties of Prickly Pear Fruit. Open Access Journal of Biogeneric Science and Research. 2021. 7(2). DOI: 10.46718/JBGSR.2021.07.000164
32. Alam-Eldein, S.M., Ennab, H.A., Omar, A.E.D.K., Omar, A.A. Harvest and Postharvest Technology of *Opuntia* spp. Opuntia spp.: Chemistry, Bioactivity and Industrial Applications. Springer. Cham, 2021. Pp. 219–255. DOI: 10.1007/978-3-030-78444-7_10
33. Mannai, F., Ammar, M., Yanez, J.G., Elaloui, E., Moussaoui, Y. Cellulose fiber from Tunisian Barbary Fig "*Opuntia ficus-indica*" for papermaking. Cellulose. 2016. 23(3). Pp. 2061–2072. DOI: 10.1007/s10570-016-0899-9
34. Castellano, J., Marrero, M.D., Ortega, Z. *Opuntia* Fiber and Its Potential to Obtain Sustainable Materials in the Composites Field: A Review. Journal of Natural Fibers. 2022. 19(15). Pp. 10053–10067. DOI: 10.1080/15440478.2021.1993479
35. Singh, A.A. Effect of Water Absorption on Interface and Tensile Properties of Jute Fiber Reinforced Modified Polyethylene Composites Developed by *Palsule* Process. Applied Polymer Composites. 2013. 1(2). Pp. 113–124.
36. Alomayri, T., Assaedi, H., Shaikh, F.U.A., Low, I.M. Effect of water absorption on the mechanical properties of cotton fabric-reinforced geopolymer composites. Journal of Asian Ceramic Societies. 2014. 2(3). Pp. 223–230. DOI: 10.1016/j.jascer.2014.05.005
37. Mohammed, M., Jawad, A.J.A.M., Mohammed, A.M., Oleiwi, J.K., Adam, T., Osman, A.F., Dahham, O.S., Betar, B.O., Gopinath, S.C.B., Jaafar, M. Challenges and advancement in water absorption of natural fiber-reinforced polymer composites. Polymer Testing. 2023. 124. Article no. 108083. DOI: 10.1016/j.polymertesting.2023.108083
38. Haigh, R., Sandanayake, M., Bouras, Y., Vrcelj, Z. A review of the mechanical and durability performance of kraft-fibre reinforced mortar and concrete. Construction and Building Materials. 2021. 297. Article no. 123759. DOI: 10.1016/j.conbuildmat.2021.123759
39. Ahmed, M., Hadi, K.M.E., Hasan, M.A., Mallick, J., Ahmed, A. Evaluating the co-relationship between concrete flexural tensile strength and compressive strength. International Journal of Structural Engineering. 2014. 5(2). Pp. 115–131. DOI: 10.1504/IJSTRUCTE.2014.060902
40. Sankar, B., Ramadoss, P. Experimental and Statistical Investigations on Alccofine Based Ternary Blended High-performance Concrete. International Journal of Engineering. 2022. 35(8). Pp. 1629–1640. DOI: 10.5829/ije.2022.35.08b.19
41. Li, Z., Li, J., Lu, W., Zhang, Y. Research Progress and Application Prospects of Plant Fibers in Geopolymer Concrete: A Review. Materials. 2025. 18(10). Article no. 2342. DOI: 10.3390/ma18102342
42. Daza-Badilla, L., Gómez, R., Díaz-Noriega, R., Avudaiappan, S., Skrzypkowski, K., Saavedra-Flores, E. I., Korzeniowski, W. Thermal Conductivity in Concrete Samples with Natural and Synthetic Fibers. Materials. 2024. 17(4). Article no. 817. DOI: 10.3390/ma17040817
43. Bessenouci, M.Z., Triki, N.B., Khelladi, S., Draoui, B., Abene, A. The Apparent Thermal Conductivity of Pozzolana Concrete. Physics Procedia. 2011. 21. Pp. 59–66. DOI: 10.1016/j.phpro.2011.10.010
44. Mydin, M.A.O. Assessment of Thermal Conductivity, Thermal Diffusivity and Specific Heat Capacity of Lightweight Aggregate Foamed Concrete. Jurnal Teknologi. 2016. 78(5). Pp. 477–482. DOI: 10.11113/jt.v78.8374

Information about the authors:

***Imeen Tarkhani**, PhD*
E-mail: imeentarkhani16@gmail.com

***Zied Kammoun**,*
ORCID: https://orcid.org/0000-0002-3000-661X
E-mail: kammounzied@yahoo.fr

***Abderraouf Trabelsi**,*
E-mail: abederraouftrabelsi@gmail.com

***Hichem Smaoui**,*
E-mail: hismaoui@yahoo.fr

Received 10.08.2025. Approved after reviewing 14.01.2026. Accepted 14.01.2026.